Physical interpretation of the correlation between multi-angle spectral data and canopy height

GEOPHYSICAL RESEARCH LETTERS, VOL. 34, L18405, doi:10.1029/2007GL031143, 2007

Physical interpretation of the correlation between multi-angle spectral data and canopy height

M. A. Schull,[1] S. Ganguly,[1] A. Samanta,[1] D. Huang,[2] N. V. Shabanov,[1] J. P. Jenkins,[3] J. C. Chiu,[4] A. Marshak,[5] J. B. Blair,[6] R. B. Myneni,[1] and Y. Knyazikhin[1]

Received 10 July 2007; revised 21 August 2007; accepted 22 August 2007; published 25 September 2007.

[1] Recent empirical studies have shown that multi-angle spectral data can be useful for predicting canopy height, but the physical reason for this correlation was not understood. We follow the concept of canopy spectral invariants, specifically escape probability, to gain insight into the observed correlation. Airborne Multi-Angle Imaging Spectrometer (AirMISR) and airborne Laser Vegetation Imaging Sensor (LVIS) data acquired during a NASA Terrestrial Ecology Program aircraft campaign underlie our analysis. Two multivariate linear regression models were developed to estimate LVIS height measures from 28 AirMISR multi-angle spectral reflectances and from the spectrally invariant escape probability at 7 AirMISR view angles. Both models achieved nearly the same accuracy, suggesting that canopy spectral invariant theory can explain the observed correlation. We hypothesize that the escape probability is sensitive to the aspect ratio (crown diameter to crown height). The multi-angle spectral data alone therefore may not provide enough information to retrieve canopy height globally. **Citation:** Schull, M. A., et al. (2007), Physical interpretation of the correlation between multi-angle spectral data and canopy height, *Geophys. Res. Lett.*, *34*, L18405, doi:10.1029/2007GL031143.

1. Introduction

[2] Canopy structure determines the amount of carbon sequestered in the vegetation pool, and incomplete knowledge of this amount contributes to the current uncertainty on predictions of future atmospheric CO_2 concentrations [*International Panel of Climate Change*, 2001]. Recent efforts using ground truth and lidar data to train MISR retrievals of vegetation structure have made significant strides toward developing a passive satellite technology for vegetation monitoring. It has been shown that multi-angle spectral data conveys information about fractional-area distributions [*Braswell et al.*, 2003; *Heiskanen*, 2006; *Chopping et al.*, 2006a, 2006b], stand basal area [*Jenkins et al.*, 2004], tree height [*Ranson et al.*, 2005; *Kimes et al.*, 2006, *Heiskanen*, 2006], forest cover density [*Nolin*, 2004] and biomass [*Baccini et al.*, 2004; *Chopping et al.*, 2007]. These results have employed the use of empirically based techniques, which are site specific and may not be extendable to operational use, given different structural and climatic conditions. Development of physically based approaches to interpret remote sensing data is therefore required not only to take full advantage of available remotely sensed data but also to advance our understanding of requirements for future space based measurements of vegetation 3D structure. In this paper, we use the concept of canopy spectral invariants to explain physics behind observed correlation between multi-angle multi-spectral data and canopy structure.

2. Canopy Spectral Invariants

[3] Photons that have entered the vegetation canopy undergo several interactions with leaves before either being absorbed or exiting the medium through its upper or lower boundary. As a result of an interaction, photons can either be scattered or absorbed by a phytoelement. The probability of the scattering event, or leaf single scattering albedo, ω_λ, depends on the wavelength and is a function of the leaf biochemical constituents. If objects are large compared with the wavelength of the radiation, e.g., leaves, branches, etc., the photon free path between two successive interactions is independent of the wavelength [*Ross*, 1981]. The interaction probabilities for photons in vegetation media, therefore, are determined by the structure of the canopy rather than photon frequency or the optics of the canopy. To quantify this feature, *Smolander and Stenberg* [2005] introduced the notion of recollision probability, p, defined as the probability that a photon scattered from a phytoelement in the canopy will interact within the canopy again. This spectrally invariant parameter is purely a function of canopy structural arrangement [*Knyazikhin et al.*, 2005; *Huang et al.*, 2007b; *Lewis and Disney*, 2007; *Mõttus*, 2007]. Additionally scattered photons can escape the vegetation canopy, either through the upper or lower boundary. Their angular distribution is given by the directional escape probability, $\rho(\Omega)$ [*Huang et al.*, 2007b].

[4] Under the assumption that the spectral invariants p and ρ remain constant in successive interactions, the bidirectional reflectance factor, $BRF_\lambda(\Omega)$, is an explicit function of spectrally invariant recollision and escape probabilities and spectrally varying single scattering albedo, ω_λ, i.e.,

$$BRF_\lambda(\Omega) = \rho(\Omega)\omega_\lambda i_0 + \rho(\Omega)\omega_\lambda^2 p i_0 + \ldots + \rho(\Omega)\omega_\lambda^m p^{m-1} i_0 + \cdots = \frac{\omega_\lambda}{1-\omega_\lambda p} R_1(\Omega). \quad (1)$$

[1]Department of Geography and Environment, Boston University, Boston, Massachusetts, USA.
[2]Atmospheric Sciences Division, Brookhaven National Laboratory, Upton, New York, USA.
[3]Complex System Research Center, University of New Hampshire, Durham, New Hampshire, USA.
[4]Joint Center for Earth Systems Technology, University of Maryland, Baltimore County, Baltimore, Maryland, USA.
[5]Climate and Radiation Branch, NASA Goddard Space Flight Center, Greenbelt, Maryland, USA.
[6]Laser Remote Sensing Laboratory, NASA Goddard Space Flight Center, Greenbelt, Maryland, USA.

0094-8276/07/2007GL031143$05.00

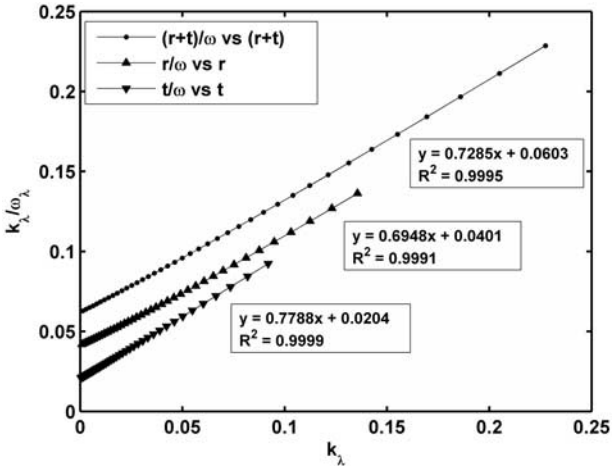

Figure 1. Canopy spectral invariants for canopy hemispherical reflectance, r_λ (upward triangle), transmittance of collided radiation, t_λ (downward triangle), and scattering coefficient $r_\lambda + t_\lambda$ (circle). By plotting values of the ratio $\kappa_\lambda/\omega_\lambda$ versus κ_λ a linear relationship is obtained. Here κ_λ represents either r_λ, t_λ, or $r_\lambda + t_\lambda$. The intercepts corresponding to r_λ and t_λ give the escape probabilities in upward (0.0401) and downward (0.0204) directions. The slope of the $(r_\lambda + t_\lambda)/\omega_\lambda$ versus $(r_\lambda + t_\lambda)$ line is an accurate estimate of the recollision probability (0.7285) [*Huang et al.*, 2007b]. Its intercept (0.0603) is the sum of the upward and downward escape probabilities. The specification of the recollision probability from the spectral reflectance-only or transmittance-only underestimates (0.6948) or overestimates (0.7788) the true value. Calculations were performed using the stochastic radiative transfer equation for a vegetation canopy consisting of identical cylindrical "trees" uniformly distributed in the canopy layer [*Huang et al.*, 2007a]. The aspect ratio, ground cover and plant leaf area index are set to 1, 0.16 and 10. The solar zenith angle and azimuth of the incident beam are 30° and 0°.

Here i_0 is the probability of initial collisions, or canopy interceptance defined as the portion of photons from the incident beam that are intercepted, i.e., collide with phytoelements for the first time. Canopy interceptance does not depend on the wavelength and is a function of the direction of incident beam and canopy structure. The term $R_1(\Omega) = \rho(\Omega)i_0$ is the escape probability expressed relative to the number of incident photons. Values of p and R_1 can be determined by fitting equation (1) to measured reflectance spectrum.

[5] In general case the recollision and escape probabilities vary with the scattering order m. For $m = 1$, the directional escape probability coincides with the bi-directional gap probability. This fundamental canopy structure parameter therefore is a special case of the directional escape probability. The probabilities, however, reach plateaus as the number of interactions m increases. Monte Carlo simulations of the radiation regime in 3D canopies suggest that the probabilities saturate after 2 to 3 photon-canopy interactions for low to moderate LAI canopies [*Lewis and Disney*, 1998]. *Huang et al.* [2007b] found that the relative error in the approximation (1) does not exceed 5% as long as the single scattering albedo is below 0.9. The use of this approximation minimally impacts the values of the escape probability. Violation of the above assumption, however, can result in a transformation of the recollision probability to its effective value as a result of fitting equation (1) to measured spectral reflectance [*Huang et al.*, 2007b]. The reader is referred to *Huang et al.* [2007b] for the current state of understanding in this field.

[6] Equation (1) is the basis for our data analyses. Specifically, we would like to show that the spectral BRF and $R_1(\Omega)$ convey comparable information about canopy structure. As such, the canopy spectral invariants, p and R_1, can explain the physics behind the observed correlation between multi-angle spectral and lidar data, where the measurable directional escape probability is the variable that imbues canopy structure dependence to multi-angle spectral data.

3. Method Used and Its Limitations

[7] Equation (1) can be rearranged to a form which we will use to obtain the spectral invariants p and $R_1(\Omega)$ from multi-angle spectral data, namely,

$$\frac{BRF_\lambda(\Omega)}{\omega_\lambda} = pBRF_\lambda(\Omega) + R_1(\Omega). \quad (2)$$

[8] By plotting the ratio $BRF_\lambda/\omega_\lambda$, versus BRF_λ, a linear relationship is obtained (Figure 1), where the slope and intercept give the recollision and escape probabilities, respectively. We will use AirMISR data (section 4) at blue, green, red and near infrared spectral bands to specify p and $R_1(\Omega)$ using equation (2).

[9] The spectral invariant relationships are formulated for a vegetation canopy (1) bounded from below by a non-reflecting surface and (2) illuminated from above by a wavelength independent parallel beam. However, we will use measured multi-angle spectral data without correcting for canopy substrate effects (i.e. the fact that observed canopies do not have totally absorbing lower boundaries), which will impact the values of $R_1(\Omega)$ [*Huang et al.*, 2007b]. The second assumption requires the use of the BRF. This assumption is not met in our research since the AirMISR BRF product was not available for all sites of the study area. We will use hemispherical-directional reflectance factor (HDRF) which characterizes surface reflective properties under ambient atmospheric condition [*Martonchik et al.*, 2000]. At shorter wavelengths the diffuse component of the incident radiation is not negligible due to Rayleigh and aerosol scattering and exhibits strong variation with the wavelength. Since the interceptance, i_0 of the vegetation canopy is higher under diffuse illumination conditions [*Tian et al.*, 2004; *Min*, 2005; *Gu et al.*, 2002, *Jenkins et al.*, 2007] the use of HDRF at blue and green spectral bands can result in a systematic overestimation of the escape probability (see auxiliary material[1]), but since it is systematic it does not effect the outcome of our results.

[10] Equation (2) requires the spectral single scattering albedo ω_λ which depends on the scale at which this quantity

[1]Auxiliary materials are available in the HTML. doi:10.1029/2007GL031143.

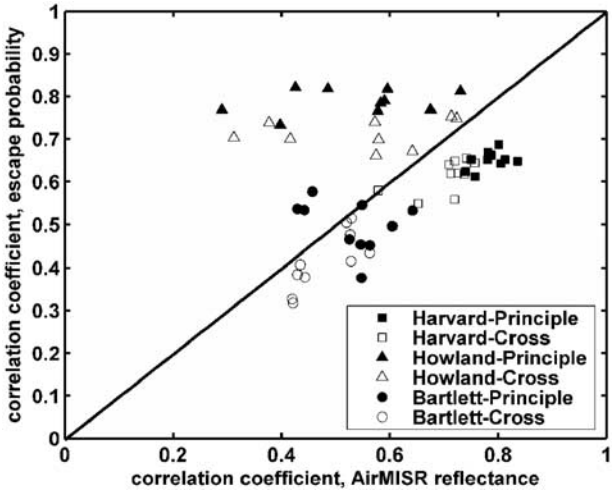

Figure 2. Correlation coefficients for escape probability predicted heights versus correlations for AirMISR predicted heights for three sites at two different observation geometries (Principle and Cross planes) and ten combinations of training and testing sets.

is defined. For example, the single scattering albedo of a needle, shoot, branch, tree crown, etc., are different. The choice of scale does not violate spectral invariant relationships [*Smolander and Stenberg*, 2005; *Lewis and Disney*, 2007] although it impacts the values of spectral invariants. We will use a leaf albedo spectrum measured during the Flakaliden field campaign [*Huang et al.*, 2007b].

[11] Violation of the above assumptions and the use of one single scattering albedo pattern for all sites impact values of the spectral invariants and result in ambiguities in the scale at which they are defined. As we will see from our analyses, however, this will have a minimal impact on the estimation of information content of the escape probability.

4. Data Used

[12] The study area consists of three locations, which encompass a transition from evergreen needle leaf to deciduous broadleaf forest (Figure S2 in the auxiliary material). Howland Forest (45.2 N, 68 0.74 W) at International Paper's Northern Experimental Forest site is characterized as an evergreen needleleaf forest. Harvard Forest (42.54 N, 72.17 W) a Long Term Ecological Research (LTER) site is classified as a mixed deciduous broadleaf and evergreen needle leaf forest. Bartlett Experimental Forest (44.06 N, 71.29 W) a USDA Forest Service site is mostly a broadleaf deciduous forest with areas of conifers at the higher elevations. Lidar and multi-angle spectral data were acquired in the summer of 2003 as part of a NASA Terrestrial Ecology Program aircraft campaign and are publicly available at https://lvis.gsfc.nasa.gov and http://eosweb.larc.nasa.gov/PRODOCS/airmisr/table_airmisr.html, respectively.

4.1. Lidar Data

[13] Airborne Laser Vegetation Instrument System (LVIS) is a pulsed laser altimeter which measures range by timing a short-10 ns duration pulse of laser light between the instrument and the target surface. LVIS point data collected from the H100 height measures (see auxiliary material) were sampled into a raster grid dataset at a 28 m nominal resolution using a window average scheme. A strong correlation between field measured and LVIS estimates of canopy height has been documented for the Bartlett and Howland sites [*Kimes et al.*, 2006; *Anderson et al.*, 2006] allowing for the use of LVIS as a surrogate for canopy height.

4.2. Multi-Angle Spectral Data

[14] The Airborne Multi-angle Imaging Spectrometer (AirMISR) instrument on NASA's ER-2 aircraft employs four channel spectral data at nine different viewing angles (See Figure S3 in the auxiliary material). Level 1 radiometrically and geometrically corrected radiance data product collected in the principle and cross-planes were converted to at-aircraft level HDRF. The data is provided in WGS 84 UTM projection and has a common ground resolution of 27.5 m with all the cameras co-registered to a common swath width of 11 km. The AirMISR dataset is resampled to 28 m resolution and co-registered to match the LVIS dataset. More information about the dataset characteristics and methods used can be found in the auxiliary material.

5. Multivariate Linear Regression Models

[15] For each study area and for each AirMISR sun-view geometry (Figure S3 in the auxiliary material), we first created a random subset (training set) from 1/3 of the AirMISR-LVIS dataset to derive two multivariate linear regression models for estimating LVIS canopy height measures. The independent variables for the first model were reflectance values of AirMISR HDRF for 4 spectral bands at 7 view directions, totaling 28 variables. To obtain the second model, we retrieved the escape probability at 7 AirMISR view angles using equation (2) first and then used the obtained values as the 7 independent variables in the model. The models were then used to predict LVIS height measure from the AirMISR HDRF and the escape probability in the remaining 2/3 of pixels (testing set). The correlation coefficients calculated using values of predicted and actual LVIS heights were employed as a measure of the information about canopy structure that AirMISR HDRF and escape probability convey. This approach was applied to AirMISR-LVIS data set degraded to 283 m resolution (see Figure S4 and associated text in the auxiliary material).

6. Results and Discussions

[16] Figure 2 shows the correlation coefficients for AirMISR predicted LVIS height estimates versus correlations for escape probability predicted LVIS heights for three sites at two different observation geometries and for ten combinations of training and testing sets. There are several important features noteworthy in the correlation coefficients. The correlation coefficient for the AirMISR predicted LVIS heights measure exhibits a higher sensitivity to the test data compared to its escape probability counterpart. The effect is most pronounced at Howland and less for Bartlett sites. This suggests that the test data should adequately represent variation in both structural and spectral

components in the case of multi-angle spectral data while the escape probability requires mainly structural information to train the model. As such, the latter is purely function of canopy structural arrangement. On average, the correlation coefficient is higher if the AirMISR data in the principal plane are used. Overall, the wavelength independent escape probability and multi-angle spectral data tend to provide a comparable amount of information about the LVIS height measure.

[17] An additional observation garnered from the research is that one cannot use single band multi-angle information to accurately measure canopy structure. The shapes of the HDRF and escape probability can be very similar (see Figure S6 in the auxiliary material). However, the use of single band multi-angle data results in a much weaker correlation as seen in a comparison of Figure 2 and Figure S7 in the auxiliary material. This is because the escape and recollision probabilities exhibit opposite tendencies in the sense that an increase in the escape probability is accompanied by a decrease in the recollision probability [*Disney et al.*, 2005]. The denominator in equation (1) therefore tends to suppress changes in R_1, lowering the sensitivity of single band data to the canopy height. This result is consistent with findings reported by *Kimes et al.* [2006] and *Heiskanen* [2006] and suggests that single band multi-angle data are not sufficient to extract canopy horizontal structure parameters. Spectral information is required to extract the spectral invariants from the measured signal [*Panferov et al.*, 2001; *Shabanov et al.*, 2003; *Knyazikhin et al.*, 2005; *Huang et al.*, 2007b]. These variables imbue canopy structure dependence to multi-angle spectral data and, therefore, are plausible to explain the observed correlation between multi-angle spectral reflectance and canopy height.

[18] The correlation between the directional escape probability and LVIS canopy heights vary with site as can be seen in Figure 2 (see vertical axis). Howland Forest (needle leaf forest) has the highest correlation, Harvard Forest (mixed forest) shows intermediate results, and Bartlett Forest (mostly a broadleaf deciduous forest with areas of conifers at the higher elevations) exhibits the lowest correlation. The most obvious feature about each site is the difference in structural heterogeneity of the upper canopy: Howland Forest has the highest heterogeneity and gives the highest correlation while Bartlett is a dense forest with a closed canopy giving it a fairly smooth surface. As a result of this observation, we hypothesize that multi-angle spectral data are actually more sensitive to the aspect ratio (crown diameter to crown height ratio) and ground cover, and that this is responsible for the observed correlations. Indeed, a multi-angle sensor sees a tree from 3 sides, front (in relation to the sensor's direction), top, and back. At nadir the sensor sees the tree's crown diameter and at the front and back the sensor sees the tree crown's approximate height. If there is no visible height as in the case of Bartlett's closed forest, then there is no ability to measure height at all. The reason why we could predict height with higher accuracies at Howland is because the forest canopy has a conical structure allowing the sensor to see the sides of the trees and thus giving aspect ratio. A simple comparison of modeled and measured escape probabilities and visual inspection of sites do not reject our hypothesis (See Figure S5 in the auxiliary material). Further research, however, is required to validate the speculatory evaluation of multi-angle data imbuing information about canopy aspect ratio.

7. Conclusions

[19] The empirical analysis of AirMISR and LVIS data support results from previous studies [*Ranson et al.*, 2005; *Kimes et al.*, 2006; *Heiskanen*, 2006] that document a strong correlation of multi-angle multi-spectral data and canopy height. We found that the canopy spectral invariants can explain the observed correlation, where the wavelength independent directional escape probability is the variable that imbues the sensitivity of MISR data to canopy height. Spectral information is essential to extract the spectral invariant parameters from the measured signal. The significance of this result to the remote sensing of 3D canopy structure is two-fold. First, the canopy spectral invariants offer a simple, accurate and physically well-justified representation of canopy reflectance where structural and radiometric components of measured signal are naturally decoupled. This allows for retrievals of canopy structural parameters with fewer assumptions compared to traditional modeling approaches where structurally and spectrally varying parameters are functionally related in a complex manner. Second, many of existing approaches require models of the bi-directional gap probability to simulate canopy reflectance. Since this parameter is a special case of the directional escape probability, its estimation from multi-angle multi-spectral reflectance is virtually independent of any particular kind of surface model and thus enables a more direct link between canopy structure and optical remote sensing data. Finally, the information gained from canopy structure will lead to more accurate inputs for land surface-models as well as provide groundwork for more accurate biomass estimation.

[20] **Acknowledgments.** This research was supported by the Jet Propulsion Laboratory, California Institute of Technology, under contract 1259071 as part of the EOS-MISR project and by NASA Headquarters under the NASA Earth and Space Science Fellowship Program grant NNX07AO41H.

References

Anderson, J., M. E. Martin, M.-L. Smith, R. O. Dubayah, M. A. Hofton, P. Hyde, B. E. Peterson, J. B. Blair, and R. G. Knox (2006), The use of waveform lidar to measure northern temperate mixed conifer and deciduous forest structure in New Hampshire, *Remote Sens. Environ.*, *105*, 248–261.

Baccini, A. M. A. Friedl, C. E. Woodcock, and R. Warbington (2004), Forest biomass estimation over regional scales using multisource data, *Geophys. Res. Lett.*, *31*, L10501, doi:10.1029/2004GL019782.

Braswell, B. H., S. C. Hagen, W. A. Salas, and S. E. Frolking (2003), A multivariable approach for mapping sub-pixel land cover distributions using MISR and MODIS: An application in the Brazilian Amazon, *Remote Sens. Environ.*, *87*, 243–256.

Chopping, M. J., L. Su, A. Laliberte, A. Rango, D. P. C. Peters, and J. V. Martonchik (2006a), Mapping woody plant cover in desert grasslands using canopy reflectance modeling and MISR data, *Geophys. Res. Lett.*, *33*, L17402, doi:10.1029/2006GL027148.

Chopping, M., L. Su, A. Laliberte, A. Rango, D. P. C. Peters, and N. Kollikkathara (2006b), Mapping shrub abundance in desert grasslands using geometric-optical modeling and multi-angle remote sensing with CHRIS/Proba, *Remote Sens. Environ.*, *104*, 62–73.

Chopping, M., L. Su, N. Kollikkathara, and L. Urena (2007), Advances in mapping woody plant canopies using the NASA MISR instrument on Terra, paper presented at IGARSS'07, Geosci. and Remote Sens. Soc., Barcelona, Spain.

Disney, M., P. Lewis, T. Quaife, and C. Nichol (2005), A spectral invariant approach to modeling canopy and leaf scattering, paper presented at 9th International Symposium on Physical Measurements and Signatures in Remote Sensing (ISPMSRS), Inst. of Geogr. Sci. and Nat. Resour. Res., Beijing.

Gu, L., D. Baldocchi, S. B. Verma, T. A. Black, T. Vesala, E. M. Falge, and P. R. Dowty (2002), Advantages of diffuse radiation for terrestrial ecosystem productivity, *J. Geophys. Res.*, *107*(D6), 4050, doi:10.1029/2001JD001242.

Heiskanen, J. (2006), Tree cover and height estimation in the Fennoscandian tundra-taiga transition zone using multiangular MISR data, *Remote Sens. Environ.*, *103*, 97–114.

Huang, D., Y. Knyazikhin, W. Wang, D. W. Deering, P. Stenberg, N. Shabanov, and R. B. Myneni (2007a), Stochastic transport theory for investigating the three-dimensional canopy structure from space measurements, *Remote Sens. Environ*, in press.

Huang, D., et al. (2007b), Canopy spectral invariants for remote sensing and model applications, *Remote Sens. Environ.*, *106*, 106–122.

International Panel of Climate Change (2001), *Climate Change 2001: Impacts, Adaptation, and Vulnerability*, Cambridge Univ. Press, Cambridge, U. K.

Jenkins, J. P., S. Ollinger, R. Braswell, M. Martin, L. Plourde, M.-L. Smith, and D. Hollinger (2004), Detecting patterns of canopy structure and carbon uptake with multi-angle remote sensing, paper presented at MISR Science Team Meeting, Jet Propul. Lab., NASA, Pasadena, Calif.

Jenkins, J. P., A. D. Richardson, B. H. Braswell, S. V. Ollinger, D. Y. Hollinger, and M.-L. Smith (2007), Refining light-use efficiency calculations for a deciduous forest canopy using simultaneous tower-based carbon flux and radiometric measurements, *J. Agric. For. Meteorol.*, *143*, 64–79.

Kimes, D. S., K. J. Ranson, G. Sun, and J. B. Blair (2006), Predicting lidar measured forest vertical structure from multi-angle spectral data, *Remote Sens. Environ.*, *100*, 503–511.

Knyazikhin, Y., A. Marshak, and R. B. Myneni (2005) Three-dimensional radiative transfer in vegetation canopies, in *Three-Dimensional Radiative Transfer in the Cloudy Atmosphere*, edited by A. Davis and A. Marshak, pp. 617–651, Springer, New York.

Lewis, P., and M. I. Disney (1998), The Botanical Plant Modelling System (BPMS): A case study of multiple scattering in a barley canopy, paper presented at IGARSS'98, Geosci. and Remote Sens. Soc., Seattle, Wash.

Lewis, P., and M. Disney (2007), Spectral invariants and scattering across multiple scales from within-leaf to canopy, *Remote Sens. Environ.*, *109*, 196–206.

Martonchik, J. V., C. J. Bruegge, and A. Strahler (2000), A review of reflectance nomenclature used in remote sensing, *Remote Sens. Rev.*, *19*, 9–20.

Min, Q. (2005), Impacts of aerosols and clouds on forest-atmosphere carbon exchange, *J. Geophys. Res.*, *110*, D06203, doi:10.1029/2004JD004858.

Mõttus, M. (2007), Photon recollision probability in discrete crown canopies, *Remote Sensing of Environment*, *110*, 176–185.

Nolin, A. W. (2004), Towards retrieval of forest cover density over snow from the Multi-angle Imaging SpectroRadiometer (MISR), *Hydrol. Processes*, *18*, 3623–3636, doi:10.1002/hyp.5803.

Panferov, O., Y. Knyazikhin, R. B. Myneni, J. Szarzynski, S. Engwald, K. G. Schnitzler, and G. Gravenhorst (2001), The role of canopy structure in the spectral variation of transmission and absorption of solar radiation in vegetation canopies, *IEEE Trans. Geosci. Remote Sens.*, *39*, 241–253.

Ranson, K. J., G. S. Sun, and D. S. Kimes (2005), Use of Lidar and Multiangle data for estimating forest heights, paper presented at MISR Science Team Meeting, Jet Propul. Lab., NASA, Pasadena, Calif.

Ross, J. (1981), *The Radiation Regime and Architecture of Plant Stands*, edited by W. Junk, 391 pp., Kluwer Acad., Norwell, Mass.

Shabanov, N. V., Y. Wang, W. Buermann, J. Dong, S. Hoffman, G. Smith, Y. Tian, Y. Knyazikhin, and R. B. Myneni (2003), Effect of foliage spatial heterogeneity in the MODIS LAI and FPAR algorithm over broadleaf forests, *Remote Sens. Environ.*, *85*, 410–423.

Smolander, S., and P. Stenberg (2005), Simple parameterizations of the radiation budget of uniform broadleaved and conifersous canopies, *Remote Sens. Environ.*, *94*, 355–363.

Tian, Y., et al. (2004), Comparison of seasonal and spatial variations of leaf area index and fraction of absorbed photosynthetically active radiation from Moderate Resolution Imaging Spectroradiometer (MODIS) and Common Land Model, *J. Geophys. Res.*, *109*, D01103, doi:10.1029/2003JD003777.

J. B. Blair, Laser Remote Sensing Laboratory, NASA Goddard Space Flight Center, Code 694, Greenbelt, MD 20771, USA. (james.b.blair@nasa.gov)

S. Ganguly, Y. Knyazikhin, R. B. Myneni, A. Samanta, M. A. Schull, and N. V. Shabanov, Department of Geography and Environment, Boston University, 675 Commonwealth Avenue, Boston, MA 02215, USA. (sganguly@bu.edu; jknjazi@bu.edu; rmyneni@bu.edu; arindam@bu.edu; schull@bu.edu; shabanov@bu.edu)

D. Huang, Atmospheric Sciences Division, Brookhaven National Laboratory, Upton, NY 11973, USA. (dhuang@bnl.gov)

J. P. Jenkins, Complex System Research Center, University of New Hampshire, Durham, NH 03824, USA. (julian.jenkins@unh.edu)

J. C. Chiu and A. Marshak, Climate and Radiation Branch, NASA Goddard Space Flight Center, Code 613.2, Greenbelt, Maryland, USA. (alexander.marshak@nasa.gov; cchiu@climate.gsfc.nasa.gov)

Auxiliary material for Paper 2007GL031143

Physical interpretation of the correlation between multi-angle spectral data and canopy height

M.A.Schull, S.Ganguly, A.Samanta, N.V. Shabanov, R. B. Myneni, Y. Knyazikhin
(Department of Geography and Environment, Boston University)
D. Huang
(Environmental Sciences Department, Brookhaven National Laboratory)
J.C. Chiu
(Joint Center for Earth Systems Technology, University of Maryland, Baltimore County)
A. Marshak
(Climate and Radiation Branch, NASA Goddard Space Flight Center)
J. P. Jenkins
(Complex System Research Center, University of New Hampshire)
J.B. Blair
(Laser Remote Sensing Laboratory, NASA/Goddard Space Flight Center)

Schull, M. A., et al. (2007), Physical interpretation of the correlation between multi-angle spectral data and canopy height, *Geophys. Res. Lett.*, *34*, L18405, doi:10.1029/2007GL031143.

Introduction

This auxiliary section includes additional information about the sites used in this study, as well as detailed information about the methods used in this study not mentioned in the main text.

Overestimation of the escape probability due to atmospheric effects

The canopy interceptance (see Eqs. 1 and 2 in the text) depends on the angular distribution of the solar radiation incident on the vegetated surface and, therefore, is a function of atmospheric condition. Factors influencing the distribution are scattering and absorption of the solar radiation in the atmosphere. The left panel of Figure S1.tif shows the bihemispherical reflectance (BHR) to canopy single scattering albedo ratio versus BHR relationship obtained from aircraft data on surface spectral reflectance acquired during a clear sky day. At wavelengths between 400 and about 500 nm, the Rayleigh scattering is a major factor causing a strong wavelength dependence of the proportion of direct and diffuse components of the incident radiation. At these wavelengths both the BHR and leaf single scattering albedo are almost constant while the term R1 in Eq. 2 varies significantly due to variation in the direct and diffuse components with wavelength. This results in a line “almost parallel” to the vertical axis. At wavelengths between 500nm and about 700nm, interaction of solar radiation with ozone, molecules and aerosols alter not only the proportion of direct and diffuse radiation but also the single scattering properties of the atmosphere. As a result, the angular distribution of the diffuse radiation becomes wavelength dependent. Under cloud-free conditions, variation in the angular distribution of the solar radiation at the surface level becomes negligible at longer wavelengths at least for applicability of the canopy spectral invariant relationships. In this example, values of BHR/w and BHR from the spectral interval between about 722 nm and 900nm lie on a single line. Its slope and intercept

give the recollision and escape probabilities. In our approach the probabilities are specified by fitting Eq. 2 to measured surface reflectance under ambient atmospheric condition at blue, green, red and near infrared spectral wavelengths (left panel of Fig. S1.tif). This leads to a deviation of BHR/w vs BHR relationship from straight line, resulting in a systematic overestimation of the intercept and thus the overestimation of the escape probability. The deviation is due to atmospheric conditions which are independent of canopy structure and were almost constant during each flight. Since the canopy interceptance is a linear function with respect to the fraction of direct beam [Wang et al., 2003] the atmospheric effects have a minimal impact on the estimation of information content from the escape probability using multivariate linear regression models. An analysis of atmospheric effects on canopy reflective and absorptive properties can be found in Wang et al. (2003).

The right panel of Figure S1.tif shows measured spectral BHR and directional-hemispherical reflectance (DHR). The latter was obtained by using Eq. 1 and the probabilities R1 and p specified from the BHR/w vs BHR line corresponding to the spectral interval between 722nm and 900 nm. The relative difference (BHR-DHR)/DHR (vertical axis on the right side) summarizes the impact of the atmosphere discussed above on the canopy reflective properties. Note that the relative difference in the interval between 400 nm and about 500 nm is inversely proportional to the forth power of the wavelength.

Site Description

A map of study areas is shown in Fig. S2.tif.

Howland Forest

Howland Forest (Latitude 45.2 N, Longitude 68 0.74W) at International Paper's Northern Experimental Forest site is characterized as a boreal-northern hardwood transitional forest, consisting of red spruce (~41%), eastern hemlock (~25%), other conifers such as balsam fir, white pine, northern white cedar (~23%), and hardwoods such as red maple and paper birch, (~11%). Within the study area the elevation changes vary by less than 135 m creating a relatively flat topographic region. Because of its glacial past the region's soils are predominantly glacial tills, with low fertility, but high in organic material yet acidic in reaction. Additional information about the site can be found at http://public.ornl.gov/ameriflux.

Harvard Forest

Harvard Forest (Latitude 42.54 N, Longitude 72.17 W) a Long Term Ecological Research (LTER) site is classified as a temperate deciduous forest with dominant species including red oak, red maple, black birch, white pine, and hemlock. Soils in the region are characterized by glacial tills acidic in nature with low fertility. The topography of the region is characterized by rolling hills, elevation ranging from 160 m to 400 m, with local relief less than 60 m. Additional information about the site can be found at http://public.ornl.gov/ameriflux.

Bartlett Experimental Forest

Bartlett Experimental Forest (Latitude 44.06 N Longitude 71.29 W) a USDA Forest Service site is mostly a broadleaf deciduous forest with areas of needleleaf in the upper elevations. There are areas of old-growth northern hardwoods with beech, yellow birch, sugar maple, and eastern

hemlock being the dominant species. Even-aged stands of red maple, paper birch, and aspen occupy sites that were once cleared. Red spruce stands cover the highest slopes. Nearly all of the Bartlett Experimental Forest is now covered by high forest. The primary forest cover type is the sugar maple-beech-yellow birch type. However, oak types are fairly common nearby on southerly and westerly slopes. This and additional information can be found at http://www.fs.fed.us/ne/durham/4155/bartlett.htm .

Data used

LVIS and AirMISR data were acquired in the summer of 2003 as part of a NASA Terrestrial Ecology Program aircraft campaign and are publicly available at https://lvis.gsfc.nasa.gov and http://eosweb.larc.nasa.gov/PRODOCS/airmisr/table_airmisr.html, respectively.

AirMISR data

The Airborne Multi-angle Imaging Spectrometer (AirMISR) instrument which is flown on NASA's ER-2 aircraft at an altitude of about 20,000 meters employs four channel spectral data. The spectral channels are 446.4 nm, 557.5 nm, 671.7 nm and 866.4 nm. The AirMISR products include a separate file for each camera angle at which data were acquired (typically 9 angles) during a single imaging run. Four cameras point in the forward directions (entitled Af, Bf, Cf, and Df in the order of increasing off-nadir angle), one points downward in the nadir (An) and four point in the aftward directions (Aa, Ba, Ca, Da). The nominal view angles of the cameras relative to the surface reference ellipsoid are 0°, ±26.1°, ±45.6°, ±60.0° and ±70.5° where signs "+" and "-" indicate forward and aftward cameras, respectively. The most oblique camera view angles are excluded from computations due to significant co-registration offsets. The available products provided by AirMISR are Level 1 (for all sites) and Level 2 (for Howland site only) products.. Level 1 AirMISR products are radiometrically and geometrically corrected radiance data. The data is output in unsigned 16 bit integer, with a radiance scaling factor provided in the metadata header file associated with the dataset (Rad_scale_factor). The spectral equivalent at air craft level reflectances are calculated according to

$$\rho(l,k) = \frac{L(l,k) \times \pi \times D^2}{E_0}$$

where indices l and k represent band and view angle, respectively. $L(l,k)$ is the radiance for each look angle and wavelength band and $E_{0,}$ the band-specific irradiance at 1 AU, is given in the metadata set as std_solar_wgted_height. D is the earth-sun distance given in AU. The radiance values are calculated by multiplying the 16 bit L1B2 data number, $DN(l,k)$, by a band-specific radiometric scale factor (called Rad_scale_factor in the AirMISR and MISR products). [Kahn et al., 2001]. Since the Level 2 product (L2AS) that includes BRF was not available for all sites, we did not use it in our analysis.

Howland Forest AirMISR data collection campaign

Two flights were conducted over the Howland Forest (Latitude 45.01 N to 45.43 N Longitude 68.35 W to 68.98 W) at International Paper's Northern Experimental Forest on August 28, 2003. The first flight (principle plane) was conducted from 15:57:03 Z to 16:06:26 Z and covered an area located at Latitude 45.00 N to 45.43 N and Longitude 68.35 W to 69.98 W. The second flight (cross plane) conducted from 16:21:58 Z to 16:31:21 Z covered an area located at Latitude

44.94 N to 45.45 N and Longitude 68.46 W to 69.05 W. Mean solar zenith angle was approximately 36º and the mean solar azimuth angle was about 356º. Meteorological conditions at the time of the flight were 90% clear, 10% cumulus, with extra cirrus clouds moving in later in sampling period.

Harvard Forest AirMISR data collection Campaign

Two flights were conducted over the Harvard Forest (Latitude 42.28 N to 42.78 N Longitude 72.45 W to 71.81 W) a Long Term Ecological Research (LTER) site on August 24, 2003. The first flight (principle plane) was conducted from 15:36:14 Z to 15:45:37 Z and covered an area located at Latitude 42.28 N to 42.78 N and Longitude 71.93 W to 72.45 W. The second flight (cross plane) conducted from 16:00:46 Z to 16:10:10 Z covered an area located at Latitude 42.33 N to 42.77 N and Longitude 71.81 W to 72.43 W. Mean solar zenith angle was approximately 35º and the mean solar azimuth angle was about 329º. Meteorological conditions at the time of the flight were mostly sunny and clear with a few high, thin cirrus clouds in the west, moving southeast. At solar noon, the high, thin cirrus clouds were directly overhead, filtering the sun slightly.

Bartlett Experimental Forest AirMISR data collection Campaign

Two flights were conducted over the Bartlett Experimental Forest (Latitude 43.79 N to 44.28 N Longitude 71.02 W to 71.59 W) a USDA Forest Service site on August 24, 2003. The first flight (principle plane) was conducted from 16:29:36 Z to 16:31:00 Z and covered an area located at Latitude 43.79 N to 44.28 N and Longitude 71.02 W to 71.59 W. The second flight (cross plane) conducted from 16:00:46 Z to 16:10:10 Z covered an area located at Latitude 43.85 N to 44.27 N and Longitude 70.92 W to 71.56 W. Mean solar zenith angle was approximately 36º and the mean solar azimuth angle was about 358º. Meteorological conditions at the time of the flight were clear, dry, cool, and breezy.

Figure S3.tif summarizes sun-view geometries for each flight.

LVIS data

Airborne Laser Vegetation Instrument System (LVIS) is a pulsed laser altimeter which measures range by timing a short-10 ns duration pulse of laser light between the instrument and the target surface. Travel time is converted to distance based on the speed of light in the atmosphere. The energy reflected from the surface area of canopy components such as foliage, trunks, twigs, and branches, at varying heights within the footprint determines the measured waveform. The total waveform is a measure of both the vertical distribution of vegetation surface area and the distribution of the underlying ground height. The LVIS system operates at altitudes up to 10 km Above Ground Level (AGL) and has a 7º potential field-of-view (PFOV), within which footprints can be randomly spaced across track. Footprint sizes from 1 to 80 m are possible, determined by the AGL altitude of the airplane and the focal length of a diverging lens in the output path [Blair et al., 1999]. The data used in this study is 20 m spaced LVIS Ground Elevation Data [Blair et al., 2006] collected during a July 2003 New England flight campaign. LVIS data product comes in three file formats, LVIS Canopy Elevation, LVIS Ground Elevation and LVIS Geolocated Waveform. This study makes use of the LVIS Ground Elevation. The Ground Elevation product uses a cumulative count scheme to get heights at H25, H50, H75, and H100, where the levels represent the percent of the total returned energy. We used H100 as the

height measure. More information for LVIS data products can be found at https://lvis.gsfc.nasa.gov/.

Analysis of Scale

An analysis of scale dependence of the correlation coefficient on data resolution was conducted according to the multivariate regression approach to LVIS-AirMISR dataset resampled to 56, 114, 228, 283, and 342 meter resolutions. The analysis showed that a resolution of 283 m consistently resulted in the highest value of the correlation coefficient (Fig. S4.tif). As a result, the datasets were later resampled to 283 meter nominal resolution and used in our further analyses. Note that a similar result was reported in Kimes et al., [2005], and Heiskenen [2006].

References

Blair, J. B., A. M. Hofton, & D. L. Rabine, (1999), The Laser Vegetation Imaging Sensor (LVIS): A medium-altitude, digitization-only, airborne laser altimeter for mapping vegetation and topography, *ISPRS Journal of Photogrammetry and Remote Sensing*, *54*, 115-122.

Blair, J. B., A. M. Hofton, & D. L. Rabine, (2006), *Processing of NASA LVIS elevation and canopy(LGE,LCE, and LGW) data products.* http://lvis.gsfc.nasa.gov.

Kahn, R., P. Banerjee, D. McDonald, and J. V. Martouchik (2001), Aerosol properties derived from aircraft multiangle imaging over Monterey Bay, *J. Geophys. Res.,106,*11977-11995.

Michalsky J., Q. Min, J. Barnard, R. Marchand, P. Pilewskie (2003), Simultaneous spectral albedo measurements near the Atmospheric Radiation Measurement Southern Great Plains (ARM SGP) central facility, *J. Geophys. Res.*, 108 (D8), 4254, doi:10.1029/2002JD002906.

Wang, Y, W. Buermann, P. Stenberg, P. Voipio, H. Smolander, T. Häme, Y. Tian, J. Hu, Y. Knyazikhin, and R. B. Myneni (2003), A New Parameterization of Canopy Spectral Response to Incident Solar Radiation: Case Study with Hyperspectral Data from Pine Dominant Forest, *Remote Sens. Environ*., 85: 304-315.

Supplementary Figures

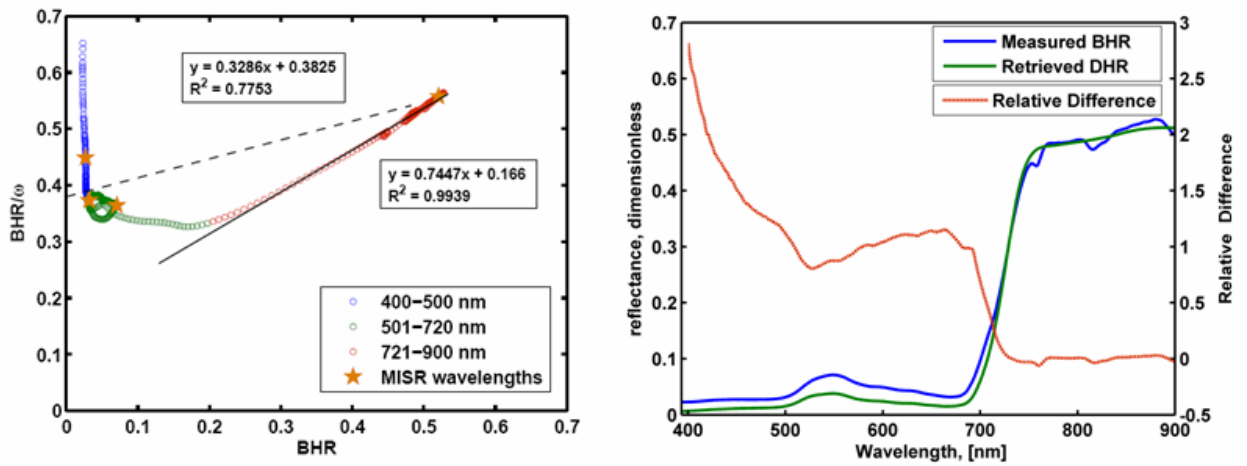

Figure S1.tif. Left Panel. Bihemispherical reflectance (BHR) to canopy single scattering albedo (w) ratio, BHR/w, versus BHR. Values of BHR/w and BHR at AirMISR spectral wavelengths and their regression line are shown as stars and a dashed line, respectively. The BHR data were collected during the Atmospheric Radiation Measurement (ARM) Enhanced Shortwave Experiment II (ARESE II) near the Central Facility (36° 36.30' W 97° 29.10') at the southern Great Plains Clouds and Radiation Testbed (CART). NASA Ames Research Center's Solar Spectral Flux Radiometer [Michalsky et al., 2003] was used to record simultaneously up- and downward spectral fluxes covering 350-1670 nm wavelength range at 1nm spectral resolution. Data were collected at a flight level of 318m. The BHR is defined as the ratio of upward to downward fluxes. The BHR values shown in the figure are the mean over records chosen given BHRs at 645nm are between a range of 0 and 0.04 and BHR values at 859 nm. greater than 0.5. Right Panel. Measured spectral BHR and DHR (vertical axis on the left side) and their relative difference (vertical axis on the right side).

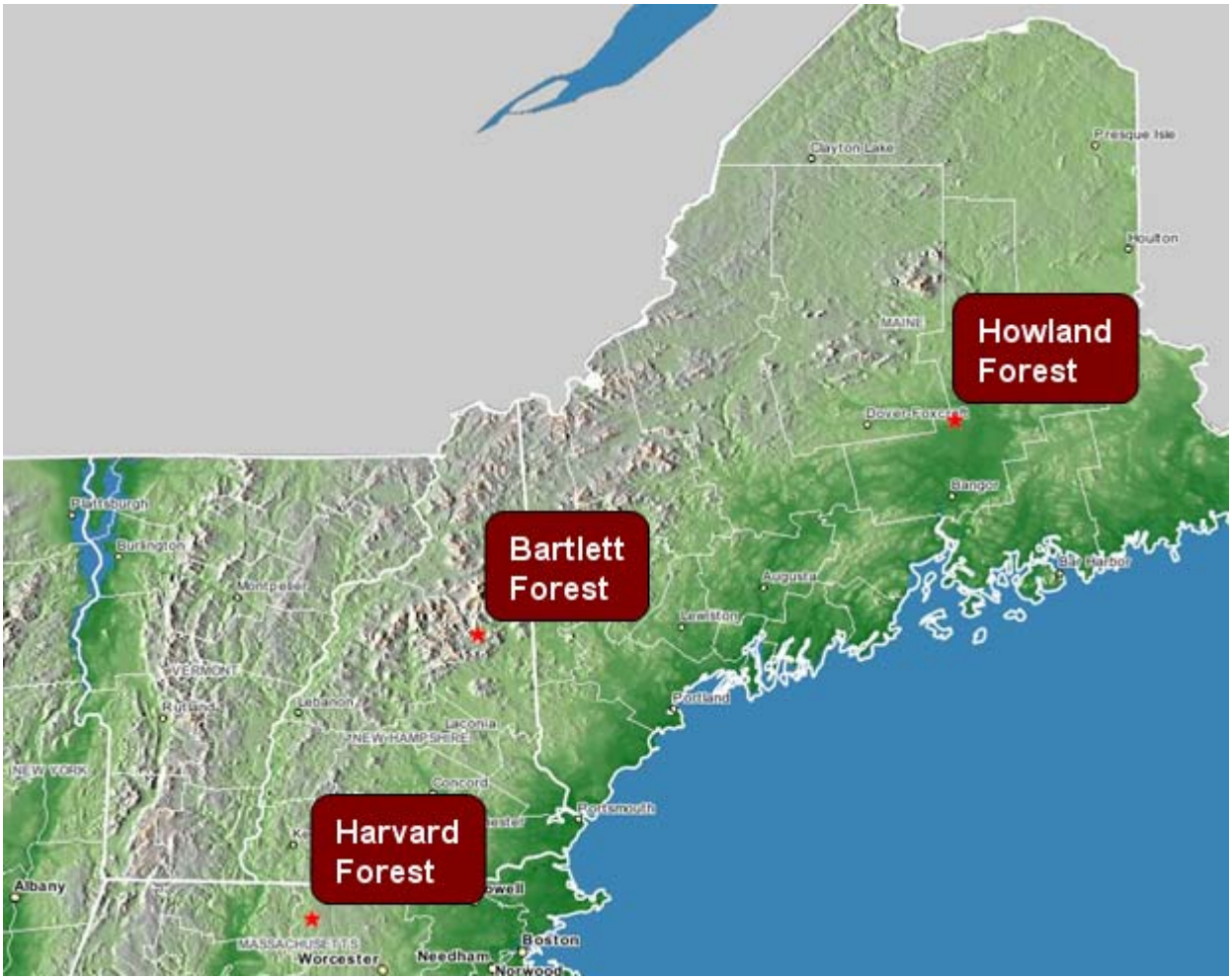

Figure S2.tif The study area consists of three locations, which encompass a transition from evergreen needle leaf to deciduous broadleaf forest. Howland Forest (Latitude 45.01 N to 45.43 N Longitude 68.35 W to 68.98 W) at International Paper's Northern Experimental Forest site is characterized as an evergreen needleleaf forest. Harvard Forest (Latitude 42.28 N to 42.78 N Longitude 72.45 W to 71.81 W) a Long Term Ecological Research (LTER) site is classified as a mixed deciduous broadleaf and evergreen needle leaf forest. Bartlett Experimental Forest (Latitude 43.79 N to 44.28 N Longitude 71.02 W to 71.59 W) a USDA Forest Service site is mostly a broadleaf deciduous forest with areas of needleleaf at the upper elevations.

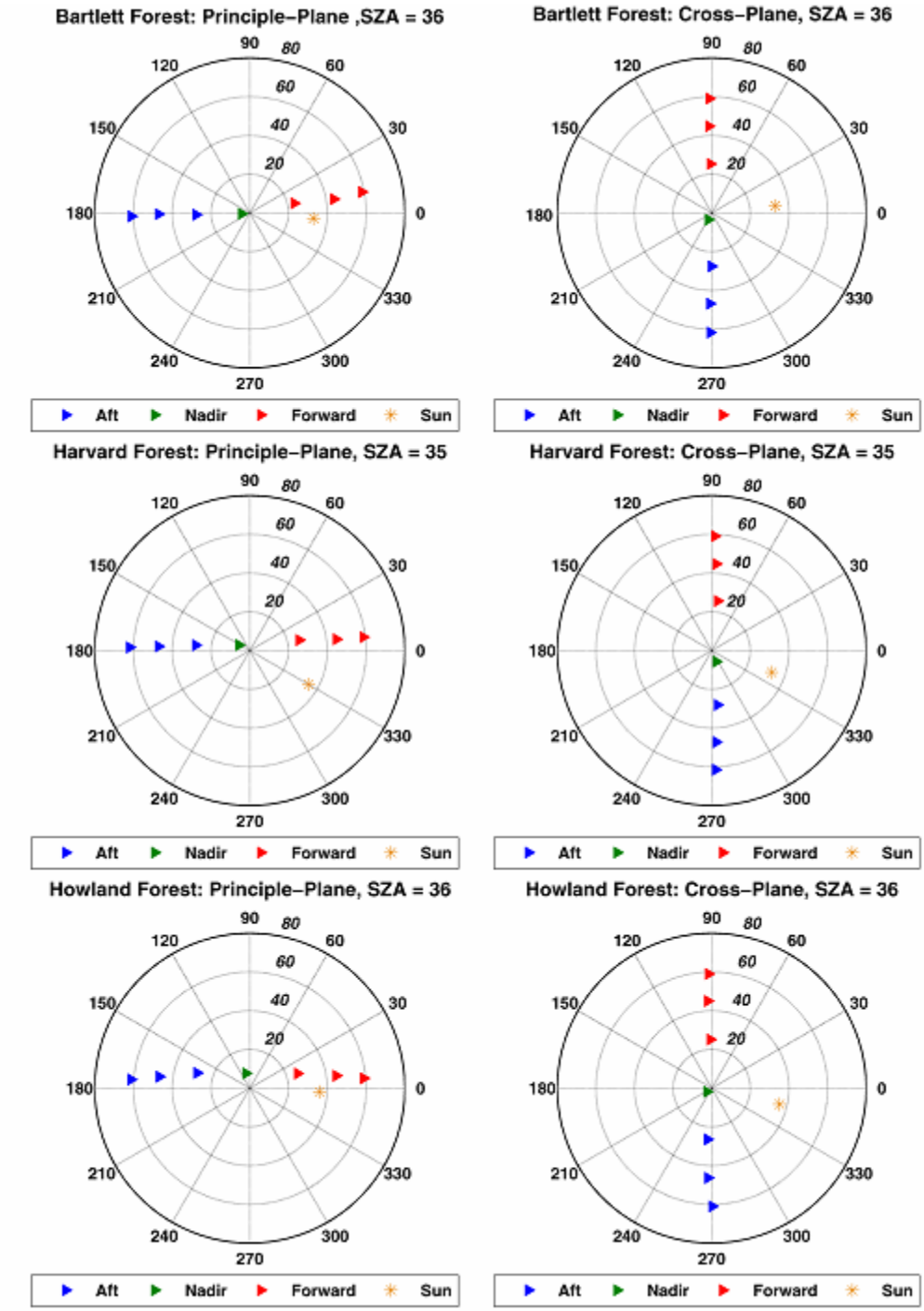

Figure S3.tif. During the NASA Terrestrial Ecology Program aircraft campaign, 2 flights were flown at each site. The left panels illustrate the sun-view geometry in the principle plane, while the right panels represent the Cross-Plane. Red, blue and green symbols correspond to forward, afterward and nadir directions, respectively. Sun position is depicted as a star.

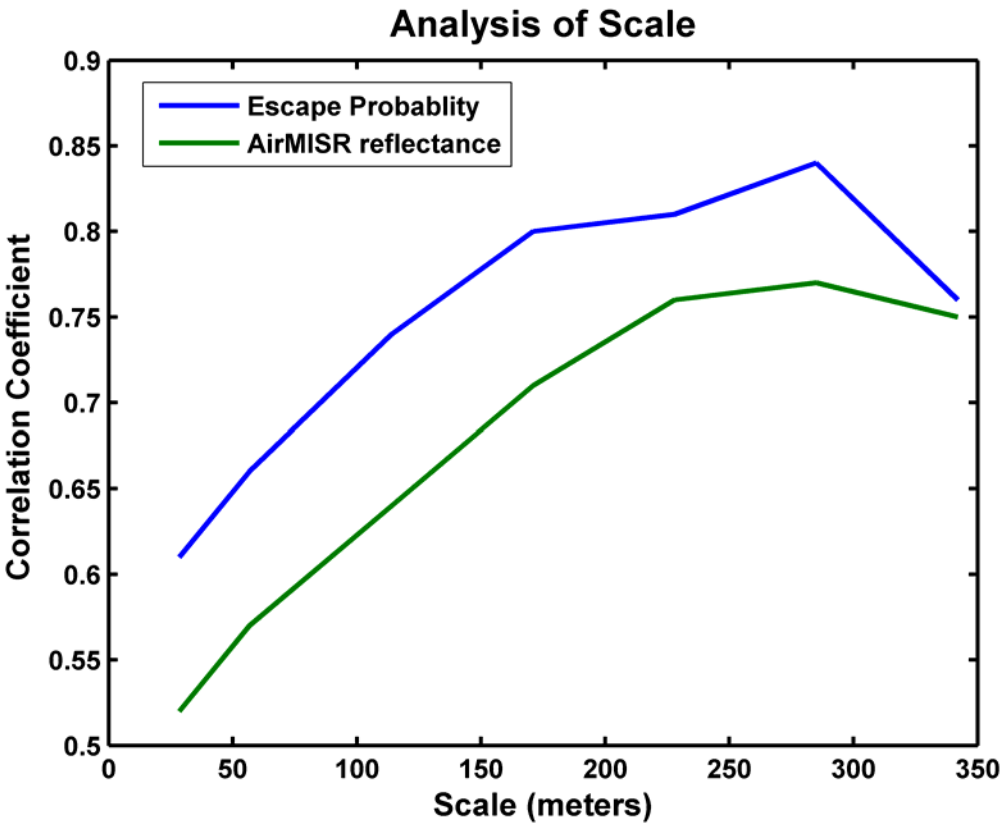

Figure S4.tif. An analysis of scale dependence of the correlation coefficient on data resolution was conducted by applying the multivariate linear regression approach to LVIS-AirMISR dataset resampled to 56m, 114m, 228m, 283m, and 342m resolution. The analysis, as seen in the figure above, showed that a resolution of 283 m consistently resulted in the highest value to the correlation coefficient.

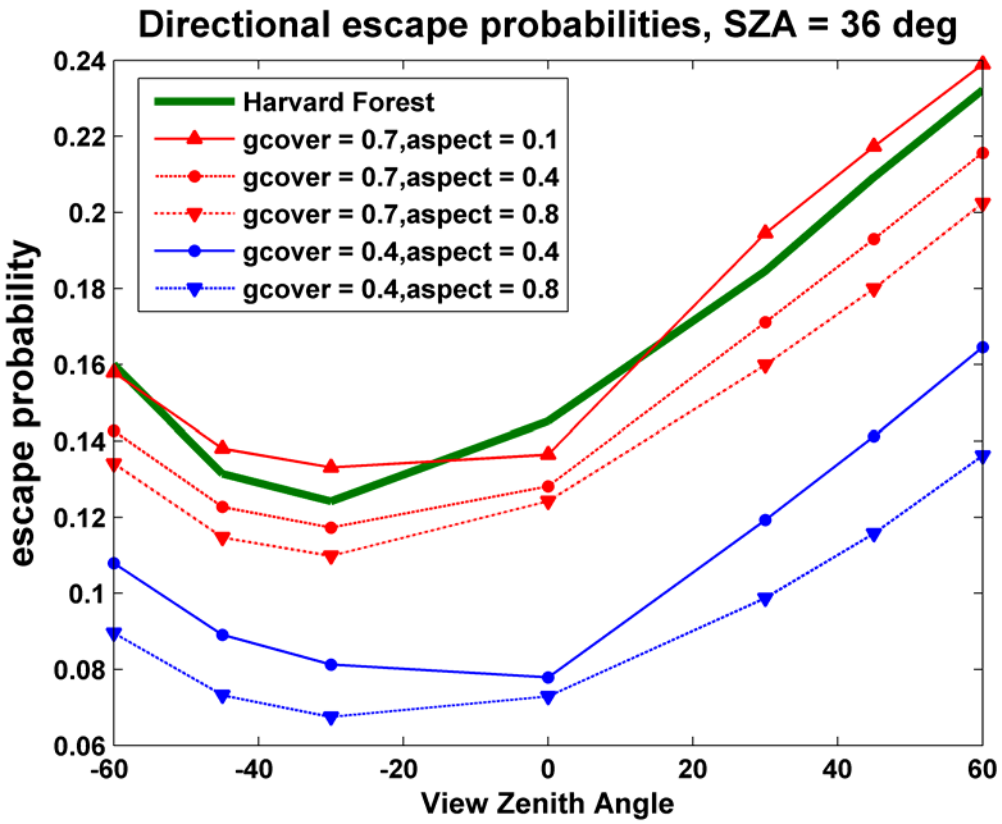

Figure S5.tif. Modeled escape probability as a function of the ground cover and aspect ratio (crown width to crown height) and escape probability derived from AirMISR data collected at Harvard Forest site are shown in the figure above. Comparison of simulated and predicted escape probabilities suggests that Harvard Forest has a low aspect ratio and high ground cover.

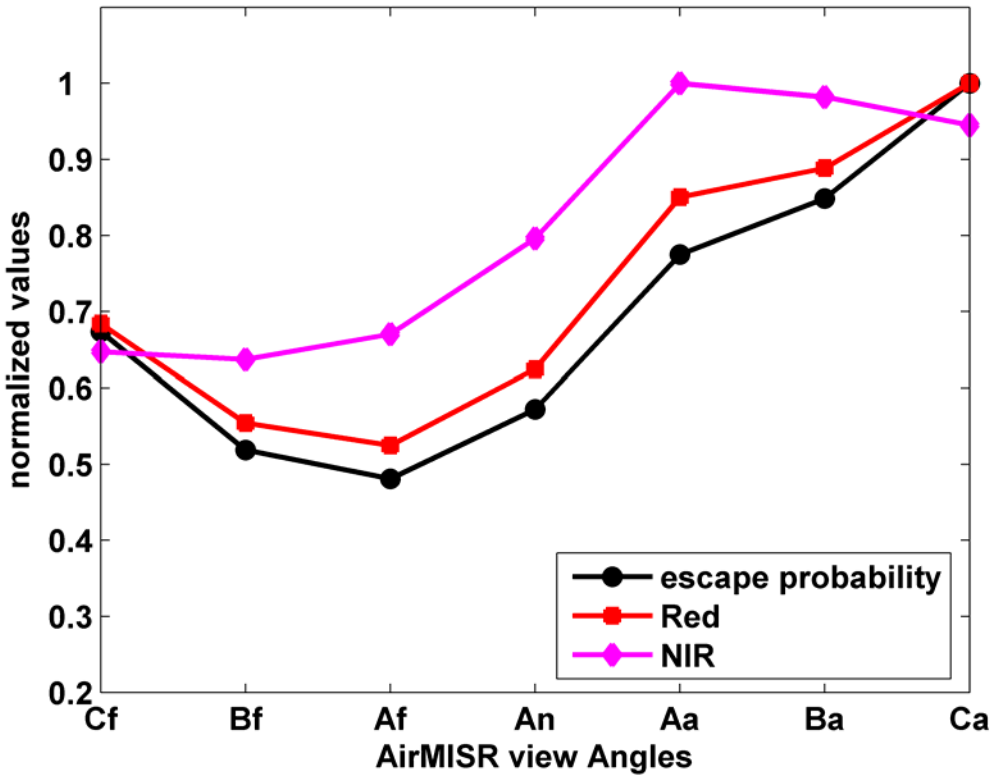

Figure S6.tif. The directional escape probability (legend "Escape probability") derived from AirMISR data using Eq. (2) from the text. AirMISR HDRF at red (legend "Red") and near-infrared (legend "NIR") spectral bands are added for comparison. The angular signatures are normalized by corresponding maximum values. Data were acquired over the Harvard Forest site. The solar zenith angle and azimuth were 35^{o} and 329^{o} respectively. The shapes of the HDRF and escape probability can be very similar e.g. as in the case of red spectral band.

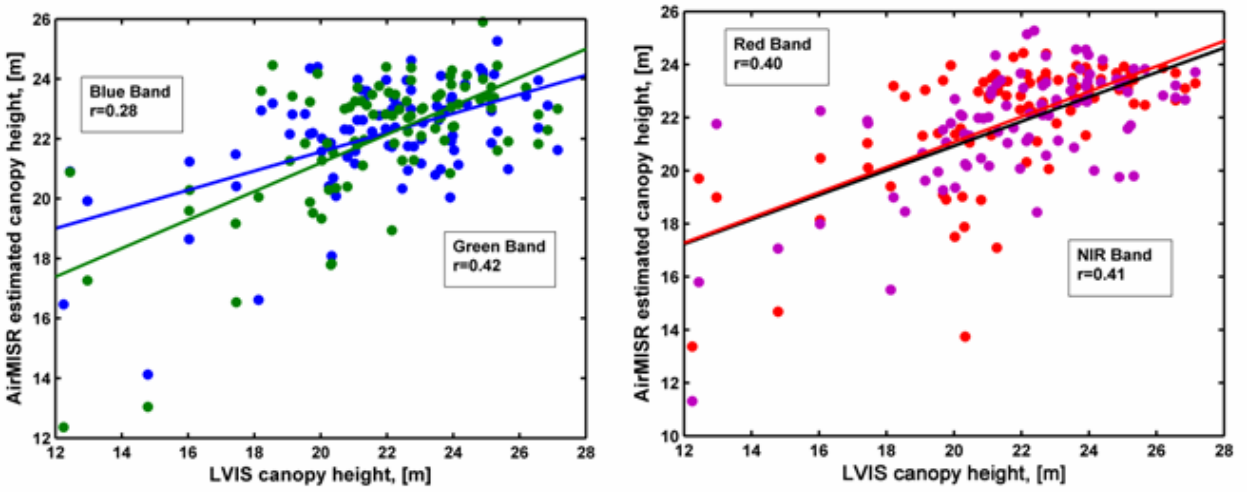

Figure S7.tif. Escape probability and HDRF at red spectral band have similar shapes as illustrated in Fig. S6.tif. One might assume that similar information about canopy structure could be obtained with the use of single band data, but looking at the figures above it is obvious that single band reflectance data will not yield very significant accuracy as seen with escape probability.